Vol 15 No 5, May 2006
1009-1963/2006/15(05)/1096-05

Chinese Physics

© 2006 Chin. Phys. Soc.
and IOP Publishing Ltd

Upconversion properties of Er^{3+}/Yb^{3+} co-doped TeO_2–Nb_2O_5–Li_2O glasses*

Su Fang-Ning(苏方宁)† and Deng Zai-De(邓再德)

Institute of Optical Communication Materials, College of Materials Science and Engineering, South China University of Technology, Guangzhou 510640, China

(Received 9 November 2005; revised manuscript received 23 February 2006)

The Er^{3+}/Yb^{3+} co-doped TeO_2–Nb_2O_5–Li_2O glass is prepared by conventional melting method, and its upconversion spectra are measured. The intense green upconversion luminescence upon excitation with a 976 nm laser diode is observed with the naked eyes. The dependence of luminescence intensity on the ratio of Yb^{3+}/Er^{3+} is discussed in detail, and the relationship between the ratio of green luminescence intensity to red luminescence intensity and the ratio of Yb^{3+}/Er^{3+} is also studied. The luminescence intensity increases with the ratio of Yb^{3+}/Er^{3+}increasing. The ratio of Yb^{3+}/Er^{3+} plays a more important role than the concentration of Er^{3+} in determining the upconversion luminescence intensity. The ratio of green luminescence intensity to red luminescence intensity reaches a maximum when ratio of Yb^{3+}/Er^{3+} is 3. Thus the glass could be one of the potential candidates for LD pumping solid-state lasers.

Keywords: upconversion, Er^{3+}/Yb^{3+} ions, tellurite glass
PACC: 7855, 7820, 4255R

1. Introduction

Rare earth doped glass has attracted much attention for many years, due to its excellent optical properties and potential applications in the fields of information process, data storage, display technology, undersea transmission and medicine.[1–6] Particularly, tellurite glass has been extensively investigated in recent years for the optical production of broad-band EDFA, TDFA and planar waveguides because of their relative low phonon energy, high refractive index, good corrosion resistance, high thermal stability and rare-earth ions solubility.[1,6,7] The study of Er^{3+}/Yb^{3+} co-doped materials[8–12] is a hot subject because Yb^{3+} has a high absorption efficiency[13,14] of 976 nm LD (laser diode) emission photons, and Er^{3+} provides an intermediate level ($^4I_{11/2}$) with long lifetime.

In this work, the tellurite glass was prepared by using a conventional melting method. Its absorption and upconversion spectra were measured. Two green emission bands centred at 523 nm and 547 nm, corresponding to the $^2H_{11/2} \rightarrow {}^4I_{15/2}$ and $^4S_{3/2} \rightarrow {}^4I_{15/2}$ transitions respectively, and one red emission band at 657 nm due to the transition of $^4F_{9/2} \rightarrow {}^4I_{15/2}$, are observed. The dependence of luminescence on the ratio of Yb^{3+}/Er^{3+} is discussed; the relationship between the ratio of green luminescence intensity to red luminescence intensity and the ratio of Yb^{3+}/Er^{3+} is also studied.

2. Experiments

2.1. Glass preparation

The starting materials for preparation Er^{3+}/Yb^{3+} co-doped glass were analytical-grade powders: TeO_2, Nb_2O_5, Li_2CO_3, Er_2O_3 and Yb_2O_3, and the glass compositions (in mol%) are $80TeO_2$–$(10-x-xR)$ Nb_2O_5–$10Li_2O$–xEr_2O_3–$xRYb_2O_3$ (x=0.1, 0.2, 0.3, 0.4 and 0.5; R represents the ratio of Yb^{3+}/Er^{3+}, R=1/5, 1/4, 1/3, 1/2, 1/1, 2/1, 3/1, 4/1 and 5/1) that are shown in Table 1.

*Project supported by the National Natural Science Foundation of China (Grant No 60307004) and the Science and Technology Program of Guangzhou, Guangdong province, China (Grant No 2004Z2-D0131).
†Corresponding author. E-mail: sufangning2003@etang.com

Table 1. The glass compositions (in molar percentage).

No.	TeO_2	Li_2O	Nb_2O_5	Er_2O_3 (x)	Yb_2O_3	R
TNL1	80	10	9.4	0.5	0.1	1/5
TNL2	80	10	9.5	0.4	0.1	1/4
TNL3	80	10	9.6	0.3	0.1	1/3
TNL4	80	10	9.7	0.2	0.1	1/2
TNL5	80	10	9.8	0.1	0.1	1/1
TNL6	80	10	9.7	0.1	0.2	2/1
TNL7	80	10	9.6	0.1	0.3	3/1
TNL8	80	10	9.5	0.1	0.4	4/1
TNL9	80	10	9.4	0.1	0.5	5/1

The very well-mixed batch was melted in an electric furnace at 850°C for 30 minutes, the glass melt was poured into a stainless mould and annealed in a muffle oven at their T_g points at a rate of 5°C/h. The annealed glass was cut into 15 mm×15 mm×1.5 mm pieces and then they were carefully polished for optical measurements.

2.2. Property measurements

The absorption spectra of the glass samples were measured with an American Perkin–Elmer–Lamda 900 UV/VIS/NIR spectrophotometer. Upconversion luminescence measurements were performed with a system of a 976 nm LD pumping and a Triax-320 spectrophotometer detector.

All the measurements were carried out at room temperature.

3. Results and discussion

3.1. Absorption spectra

The absorption spectra are shown in Fig.1, in which there appear seven absorption bands: the absorption peaks are centred at 486 nm, 521 nm, 546 nm, 657 nm, 808 nm, 977 nm and 1533 nm respectively. The energy level diagram of Er^{3+}/Yb^{3+} is shown in Fig.2, where the data of the energy levels wavenumbers for the absorption spectra were cited from Ref.[15]. The seven absorption bands stem from the transitions of $^4I_{15/2}$ (Er^{3+}) → $^4F_{7/2}$ (Er^{3+}), $^4I_{15/2}$ (Er^{3+}) → $^2H_{11/2}$ (Er^{3+}), $^4I_{15/2}$ (Er^{3+}) → $^4S_{3/2}$ (Er^{3+}), $^4I_{15/2}$ (Er^{3+}) → $^4F_{9/2}$ (Er^{3+}), $^4I_{15/2}$ (Er^{3+}) → $^4I_{9/2}$ (Er^{3+}), $^4I_{15/2}$ (Er^{3+}) → $^4I_{11/2}$ (Er^{3+})& $^2F_{7/2}$ (Yb^{3+}) → $^2F_{5/2}$ (Yb^{3+}) and $^4I_{15/2}$ (Er^{3+}) → $^4I_{13/2}$ (Er^{3+}). There exists the absorption peak at 977 nm, which is resonance absorption with the 976 nm incident photons. So we used the 976 nm LD to pump the samples. Compared with the 977 nm absorption band of Er^{3+} single doped material (Fig.3), the corresponding absorption bands of Er^{3+}/Yb^{3+} co-doped matrix are very intense, this is because Er^{3+}/Yb^{3+} co-doped matrix has a bigger absorption cross-section. As shown in Fig.1, the 977 nm absorption bands become more and more predominant in the sequence of TNLn (n=1, 2, 3, 4, 5, 6, 7, 8 and 9). That is to say, the 977 nm absorption band is becoming more and more significant with the ratio of Yb^{3+}/Er^{3+} increasing from 1/5 to 5/1, which is due to the transition of $^2F_{7/2}(Yb^{3+})$ →$^2F_{5/2}(Yb^{3+})$ with a high absorption efficiency. Take TNL9 and TNL8 for example (see Fig.4), the absorption integral area and peak's height of TNL9 are larger than those of TNL8.

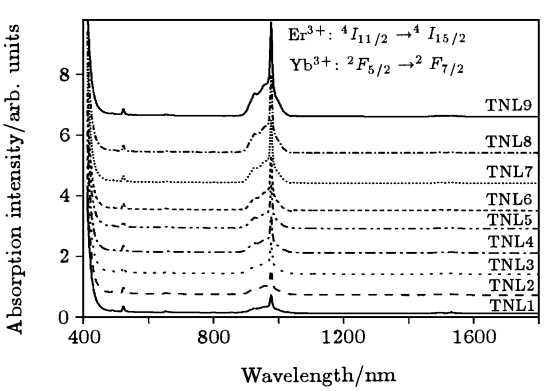


Fig.1. The absorption spectra of TNL glass.

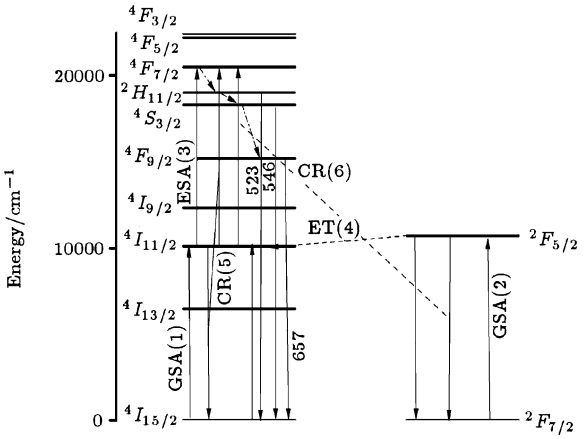


Fig.2. The simple energy level diagram of Er^{3+}/Yb^{3+} co-doped TNL glasses.

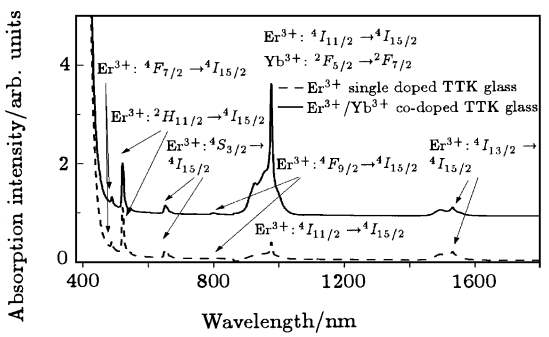


Fig.3. Comparison of the absorption spectra of Er^{3+}/Yb^{3+} co-doped with those of Er^{3+} single doped tellurite glass.

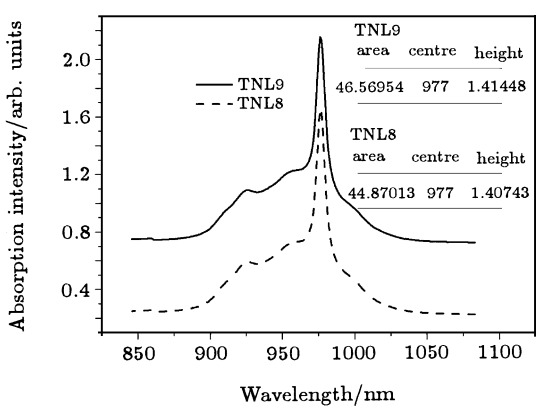


Fig.4. The 977 nm absorption cross-sections of TNL9 and TNL8. The calculated integral areas and heights are shown.

3.2. Upconversion spectra

The upconversion spectra of TNL are shown in Fig.5, where there exist three emission bands in a visible light range, at 523 nm, 546 nm and 657 nm respectively. Figure 6 shows the intensity of 546 nm emission luminescence as a function of excitation power, they are all the plots of $\log(I_{\rm up})$ versus $\log(I_{\rm IR})$. These results suggest that the $^2H_{11/2}$ level is populated through a two-photon step process. The upconversion processes[9−11,16−18] can be described as the following:

$$\text{GSA}: {}^4I_{15/2}(\text{Er}^{3+}) + h\upsilon_0 \rightarrow {}^4I_{11/2}(\text{Er}^{3+}), \quad (1)$$

$${}^2F_{7/2}(\text{Yb}^{3+}) + h\upsilon_0 \rightarrow {}^2F_{5/2}(\text{Yb}^{3+}), \quad (2)$$

$$\text{ESA}: {}^4I_{11/2}(\text{Er}^{3+}) + h\upsilon_0 \rightarrow {}^4F_{7/2}(\text{Er}^{3+}), \quad (3)$$

$$\text{ET}: {}^2F_{5/2}(\text{Yb}^{3+}) + {}^4I_{15/2}(\text{Er}^{3+}) \rightarrow {}^2F_{7/2}(\text{Yb}^{3+}) + 4I_{11/2}(\text{Er}^{3+}), \quad (4)$$

$$\text{CR}: {}^4I_{11/2}(\text{Er}^{3+}) + {}^4I_{11/2}(\text{Er}^{3+}) \rightarrow {}^4F_{7/2}(\text{Er}^{3+}) + {}^4I_{15/2}(\text{Er}^{3+}), \quad (5)$$

$${}^2F_{5/2}(\text{Yb}^{3+}) + {}^4I_{11/2}(\text{Er}^{3+}) \rightarrow {}^2F_{7/2}(\text{Yb}^{3+}) + {}^4F_{7/2}(\text{Er}^{3+}). \quad (6)$$

As has been discussed in Section 3.1, the Yb^{3+} 977 nm absorption becomes more and more predominant with the ratio of Yb^{3+}/Er^{3+} increasing. So the ET (energy transfer) mechanism should be more dominant: that is to say, the process (Eqs.(2), (4) and (6)) should be more dominant with the ratio of Yb^{3+}/Er^{3+} increasing. Referring to Fig.2 (the above mentioned processes are all marked in Fig.2), due to the resonance absorption at 976 nm, Yb^{3+} ions strongly absorb the incident photons of 976 LD, A Yb^{3+} ion transits from the ground state $^2F_{7/2}$ to the excited state $^2F_{5/2}$, then the excited Yb^{3+} transfers its energy to Er^{3+} through ET process shown by Eq.(4), thus causing the Er^{3+} ion to be excited from its' ground state $^4I_{15/2}$ to the excited state $^4I_{11/2}$; the Er^{3+} ion at $^4I_{11/2}$ can be further excited to $^4F_{7/2}$ through the CR process shown by Eq.(6). Since the lifetime of Er^{3+} ions at $^4F_{7/2}$ is short, it relaxes rapidly to the $^2H_{11/2}$ via non-radiative transition. Similarly, those Er^{3+} ions at the $^2H_{11/2}$ level may also non-radiatively relax to $^4S_{3/2}$ level, and then from $^4S_{3/2}$ level to $^4F_{9/2}$ level. When the ions at the $^2H_{11/2}$ level radiatively relax to the ground level $^4I_{15/2}$, they emit the 523 nm green luminescence. Similarly, the ions at levels $^4S_{3/2}$, and $^4F_{9/2}$ transit to the ground level $^4I_{15/2}$, they respectively emit the 546 nm and 657 nm upconversion luminescences.

The relationship between the upconversion luminescence intensity and the ratio of Yb^{3+}/Er^{3+} is shown in Fig.7, where the 523 nm, 546 nm and 657 nm emission intensities increase as R increases. Therefore the ratio of Yb^{3+}/Er^{3+} plays a more important role than the concentration of Er^{3+} in determining the upconversion luminescence intensity. The trend can be

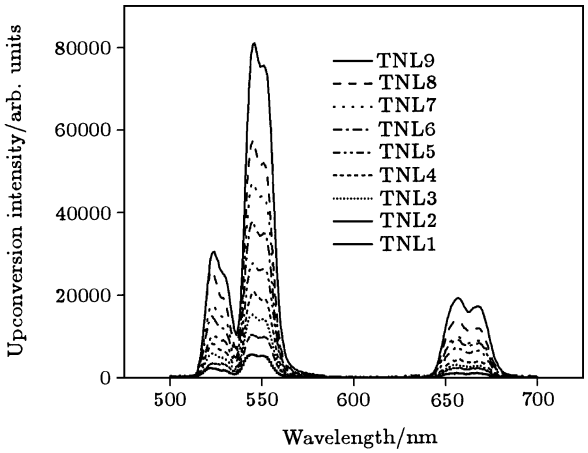


Fig.5. Upconversion luminescence spectra of Er^{3+}/Yb^{3+} co-doped TNL glass excited by 976 nm LD at a pumping power of 800mw.

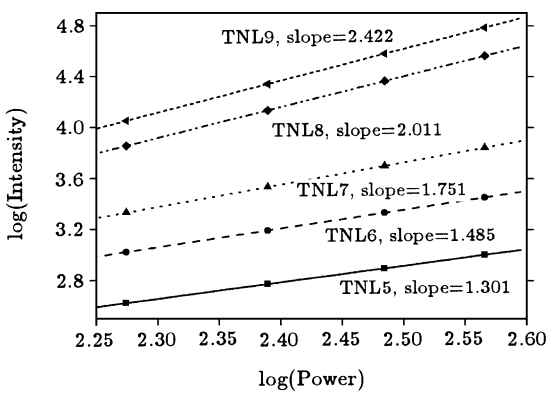


Fig.6. The 546 nm upconversion luminescence intensity of TNLn (n=5, 6, 7, 8 and 9) vs pump power. They are shown in double-log arithmetic coordinates. The pump power is in unit of mW.

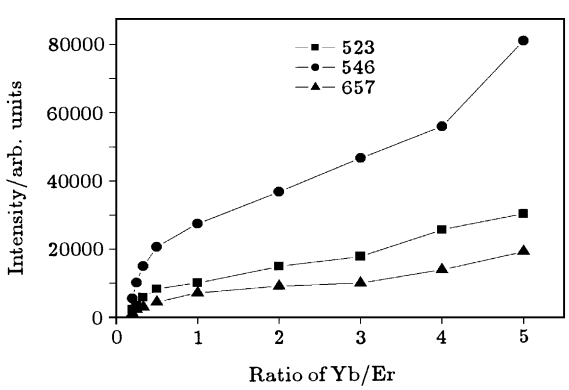


Fig.7. The dependence of upconversion luminescence intensity on R (ratio of Yb^{3+}/Er^{3+}).

obviously seen from Fig.5 and Fig.7. Particularly, from TNL5 to TNL9, the upconversion luminescence increases rapidly with R increasing.

In order to search after an excellent candidate for LD pumping solid-state lasers, especial blue-green lasers, the relationship between the ratio of green luminescence intensity to red luminescence intensity and the ratio of Yb^{3+}/Er^{3+} is studied in detail. Such a dependent relationship is shown in Fig.8, where it is clearly indicated that a maximum does appear. When R=3/1, the ratio of green luminescence intensity to red luminescence intensity reaches a maximum. Thus the glass could be one of the potential candidates for LD pumping solid-state lasers.

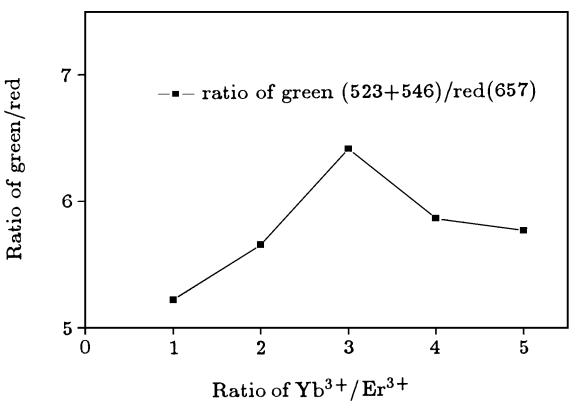


Fig.8. The relationship between the ratio of green luminescence intensity to red luminescence intensity and the ratio of Yb^{3+}/Er^{3+}.

4. Conclusions

The Er^{3+}/Yb^{3+} co-doped TeO_2–Nb_2O_5–Li_2O (TNL) is prepared by use of a conventional melting method, and its absorption spectra and upconversion spectra are measured. The intense green upconversion luminescence can be observed in all the samples with naked eyes, which manifests their potential advantages in the application of LD pumping solid-state lasers. The dependences of upconversion luminescence on the Er^{3+} concentration and the ratio of Yb^{3+}/Er^{3+} are studied in detail. The upconversion luminescence intensities increase as R increases, and the ratio of Yb^{3+}/Er^{3+} plays a more important role than the concentration of Er^{3+} in determining the upconversion luminescence intensity. The ratio of green luminescence intensity to red luminescence intensity reaches a maximum when R=3/1 in our work.

References

[1] Wei L, Li S G, Huang G S, Hu L L and Jiang Z H 2004 *Chin. Phys.* **13** 258

[2] Yeh D C, Sibley W A, Suscavage M and Drexhage M G 1987 *J. Appl. Phys.* **62** 266

[3] Ohta T, Takenaga M, Akahira N and Yamashita T 1982 *J. Appl. Phys.* **53** 8497

[4] Takenga M, Yamada N, Nishiuchi K, Nobuo A, Ohta T and Nakamura S 1983 *J. Appl. Phys.* **54** 5376

[5] Kuhaili M F A, Durrani S M A, Khawaja E E and Shirokoff J 2002 *J. Phys.* D: *Appl. Phys.* **35** 910

[6] Su F N, Deng Z D and Jiang Z H 2005 *J. Funct. Mater.* **36** 655 (in Chinese)

[7] Chen B Y, Liu Y H, Chen D D and Jiang Z H 2005 *Acta Phys. Sin.* **54** 2374

[8] Xiao S G, Yang X L and Liu Z W 2002 *Chin. Phys.* **11** 188

[9] Yang Z M, Xu S Q, Hu L L and Jiang Z H 2004 *J. Alloys Comp.* **370** 94

[10] Chen X B, Li M X, Sawanoboni N, Zeng Z and Nie Y X 2000 *Acta Phys. Sin.* **49** 2482

[11] Chen X B, Nie Y X, Du W M and Sawanoboni N 2000 *Optics Commun.* **184** 289

[12] Li T, Zhang Q Y, Zhao C, Feng Z M, Deng Z D and Jiang Z H 2005 *Chin. Phys.* **14** 1250

[13] Chen X B, Deng Z W, Sawanobori N, Meng C, Zhang G Y and Li M X 2000 *Chin. Phys.* **9** 379

[14] Liu Z W, Yang H X, Yang X L, Yuan F C and Xiao S G 2003 *Spectroscopy and Spectral Analysis* **23** 846 (in Chinese)

[15] Carnall W T, Fields P R and Rajnak K 1968 *J. Chem. Phys.* **49** 4424

[16] Vetrone F, Boyer J C, Capobianco J A, Speghini A and Bettinelli M 2004 *J. Appl. Phys.* **96** 661

[17] Yang J H, Dai N L, Dai X Q, Wen L, Hu L L and Jiang Z H 2003 *Chem. Phys. Lett.* **376** 671

[18] Choi Y G, Park B J and Kim K H 2002 *Chem. Phys. Lett.* **354** 69